International Symposium
On Turbulence and Shear Flow
Phenomena (TSFP-9)
June 30 - July 3, 2015 *Melbourne, Australia*

REYNOLDS STRESS MEASUREMENTS IN A PLANE TURBULENT WALL JET ON A SMOOTH SURFACE

Zhujun Tang
Department of Mechanical Engineering
University of Saskatchewan
57 Campus Drive, Saskatoon, Saskatchewan, Canada, S7N 5A9
nori.rostamy@usask.ca

Donald J. Bergstrom
Department of Mechanical Engineering
University of Saskatchewan
57 Campus Drive, Saskatoon, Saskatchewan, Canada, S7N 5A9
don.bergstrom@usask.ca

James D. Bugg
Department of Mechanical Engineering
University of Saskatchewan
57 Campus Drive, Saskatoon, Saskatchewan, Canada, S7N 5A9
jim.bugg@usask.ca

David Sumner
Department of Mechanical Engineering
University of Saskatchewan
57 Campus Drive, Saskatoon, Saskatchewan, Canada, S7N 5A9
david.sumner@usask.ca

ABSTRACT

The present paper documents an experimental investigation of the fluctuating velocity fields in a plane wall jet on a smooth surface using Particle Image Velocimetry. Analysis of the Reynolds stress components normalized by outer and inner scales indicates that in terms of the fluctuating velocity fields, the outer and inner layers exhibit distinct self-similar structures. Comparisons between the present results and other LDA and HWA studies for a plane wall jet on a smooth surface reveal similar behaviours for the Reynolds stress profiles. However, the magnitudes and the wall-normal locations of the peak values of the Reynolds stresses are different from previous studies, possibly due to the difference in slot Reynolds numbers.

INTRODUCTION

The plane turbulent wall jet is a flow with many important practical applications in industry. It also retains great importance in theoretical studies. Figure 1 gives a schematic of a plane wall jet, where H is the jet exit slot height, and x, U, u' and y, V, v' are the coordinate distance, mean velocity and fluctuating velocity components in the streamwise and wall-normal directions, respectively. U_m is the local maximum mean velocity and y_m is the corresponding wall-normal (y) location. As shown here, a wall jet is generally characterized by an inner region extending from the wall up to y_m that closely resembles a boundary layer, and an outer region stretching from y_m to the outer edge of the jet that is similar to a free jet. The parameter $(y_{1/2})_{out}$ denotes the wall-normal location where $U = U_m / 2$ occurs in the outer region.

The interaction between the inner and outer regions of the plane turbulent wall jet and how these two regions reach equilibrium with each other have not yet been fully resolved. Typically, scaling laws have been used to explore this issue. Wygnanski *et al*. (1992) were among the first to measure the turbulent intensities in a plane turbulent wall jet on a smooth surface. Their hot-wire anemometry (HWA) data show no collapse of the streamwise normal Reynolds stress in the outer layer of the wall jet when normalized by the outer scales at downstream distances ranging from $60H$ to $120H$ for the two slot Reynolds numbers of $Re_o = 5\times10^3$ and $Re_o = 19\times10^3$. They attributed this to a lack of

equilibrium caused by the viscous friction at the wall. Abrahamsson *et al*. (1994) reported similarity for the streamwise Reynolds stress profiles when normalized by outer scales at downstream distances of x/H = 70, 125 and 150 for three slot Reynolds number of $\mathrm{Re}_o = 1\times10^4$, 1.5×10^4 and 2×10^4. Their HWA data also shows the collapse of the wall-normal Reynolds stress profiles and the Reynolds shear stress profiles at x/H = 70, 125 and 150 for the slot Reynolds number of 1×10^4 when normalized by outer scales U_m and $(y_{1/2})_{out}$. Eriksson *et al.* (1998) acquired high-resolution laser Doppler anemometry (LDA) data in a plane wall jet at a slot Reynolds number of 9600 and found that in the outer layer of the wall jet the Reynolds stresses normalized by the outer scales increase in the streamwise direction downstream of x/H = 70. They suggested this was due to the influence of the return flow created in the experimental facility. In order to exclude this effect, they assumed the erroneous turbulence to be equal to the measured variance outside the wall jet and then subtracted this variance from each Reynolds stress measured in the outer layer. By using this correction, their Reynolds stress profiles achieved reasonable collapse up to x/H = 150. George *et al*. (2000) conducted a detailed theoretical analysis on the scaling issues of the plane turbulent wall jet based on the experimental data of Abrahamsson *et al*. (1994). They concluded that the outer scales U_m and $(y_{1/2})_{out}$ collapse the normal Reynolds stress profiles but fail to collapse the Reynolds shear stress profiles. However, substituting the inner velocity scale U_τ for the outer scale U_m does collapse the Reynolds shear stress but not the normal Reynolds stress components. Rostamy *et al*. (2011a) were among the first to conduct a thorough experimental investigation on the mean and turbulence velocity fields in a plane turbulent wall jet on both a smooth and a transitionally rough surface using LDA. They observed reasonable collapse of the Reynolds stresses profiles up to x/H = 70 for the smooth surface without the need to specifically exclude the effect of a return flow. Compared with previous studies, their results showed a similar behaviour for the Reynolds stress profiles, but with higher peak magnitudes which were attributed to the lower slot Reynolds number. On the numerical study side, Dejoan and Leschziner (2005) performed a large eddy simulation of a plane turbulent wall jet on a smooth surface for a limited domain extending 22 slot heights downstream. They reported the budgets for the turbulence kinetic energy and Reynolds stresses, which revealed a strong transport of energy by turbulent diffusion into the interaction zone where the inner and outer layers overlapped, indicative of a strong coupling between the inner and outer layers.

Based on the summary literature review given above, for a plane turbulent wall jet on a smooth surface the self-similarity of the Reynolds stresses fields, as well as related scaling issues, warrant further investigation. In addition, the effect of the slot Reynolds number on the peak values of the Reynolds stresses has not yet been resolved. Therefore, the main objective of the present study is to investigate the self-similarity of the Reynolds stress fields in a plane turbulent wall jet on a smooth surface based on a new set of PIV measurements.

EXPERIMENTAL FACILITY

The measurements were conducted with a Particle Image Velocimetry (PIV) system in the same facility used by Rostamy *et al*. (2011a), Rostamy *et al*. (2011b) and Rostamy *et al*. (2010). The water flow was supplied by a pump which discharged through a rectangular slot at an exit velocity of approximately U_0 = 1.12 m/s and U_0 = 2.24 m/s for the two flow rates considered, corresponding to slot Reynolds numbers of Re_o = 7250 (hereafter referred to as the Low Flow Rate (LFR) condition) and Re_o = 14400 (hereafter referred to as the High Flow Rate (HFR) condition). The jet exit slot had a width of W = 750 mm and height of H = 6 mm, so that the width-to-height ratio was sufficiently large to ensure that the plane wall jet was two-dimensional. The turbulence intensity in the central region of the jet at x = 0 was less than 3% for both flow rates.

Velocity measurements were carried out at different streamwise positions measured from the jet exit up to $x = 110H$ with a water temperature around T = 23.5 °C. The estimation of the measurement uncertainty followed the approach of Shinneeb (2006) and Dunn (2010). The uncertainty of the mean velocity and normal Reynolds stresses measurements was 3.6%, while the uncertainty in the Reynolds shear stress measurements was 7.2 %.

RESULTS AND DISCUSSION

1. MEAN VELOCITY FIELD

Since the outer and inner scales were determined from the mean velocity profiles and were then used to scale the Reynolds stress components, it is worthwhile to first briefly discuss the characteristics of the mean velocity field.

Figure 2 gives the mean (streamwise) velocity profile normalized by the outer scale. The corresponding data obtained by Rostamy *et al*. (2011a) and Eriksson *et al*. (1998) were also included for comparison: the present results for the mean velocity field are in good agreement with previous studies. For both flow rates considered in the present study, the wall jet was found to be fully developed in the region $40 \le x/H \le 110$. Self-similarity of the mean velocity field is clearly evident. Note that there is larger deviation among the profiles near the outer edge of the wall jet where the measurement uncertainty became higher.

To determine the friction velocity, the present mean velocity data was fitted to the classical logarithmic-law in the overlap region of the wall jet. Figure 3 shows examples of the fitted mean velocity profiles for the LFR scaled using the inner scales. As shown in this figure, the experimental data for the mean velocity generally collapse well with the log-law profile in the overlap region of the wall jet, although

there is a slight upward shift. Figure 3 includes a representative composite profile at x/H = 70 with a local Reynolds number of $y^+_{1/2}$ = 1185 $\left(y^+_{1/2} = (y_{1/2})_{\text{out}} u_\tau / \upsilon\right)$.

The magnitude of the outer spread rate, S_u, which is defined as $S_u = dy_{1/2}/dx$, was found to be S_u = 0.0827 and 0.0722 for the LFR and HFR conditions, respectively. For comparison, Rostamy *et al*. (2011a) found the spread rate to be 0.0791, and Eriksson *et al*. (1998) obtained a spread rate of 0.0782 at a slot Reynolds number of Re_o = 9600, while Tachie *et al*. (2004) reported a spread rate of 0.085 for the largest slot Reynolds number of Re_o = 12500 and 0.090 for the lowest slot Reynolds number of Re_o = 6000. The present values are reasonably close to those of Rostamy *et al*. (2011a) (4.6% difference) as well as to the result of Eriksson *et al*. (1998) (5.8% difference). In addition, as Tachie *et al*. (2004) also concluded, the present spread rates show a dependence on the slot Reynolds number, which was also observed by many previous studies. The decay rate of the maximum velocity in the power-law relation used by Barenblatt *et al*. (2005) was calculated to be -0.545 and -0.551 for the LFR and HFR, respectively, which, if taking the slot Reynolds number dependence effect into account, are in reasonable agreement (less than 9% difference) with the value of -0.6 reported in their study.

Figure 4 shows the skin friction coefficient C_f ($C_f = 2(U_\tau/U_m)^2$, where U_τ is the local friction velocity and U_m is the local maximum mean velocity) based on the present measurements as well as the values obtained by several previous studies, which compare favourably with the present results. This provides additional confidence in the values obtained for the friction velocity, which was used to obtain the inner length and velocity scales.

2. FLUCTUATING VELOCITY FIELD

2.1 Correction of the Reynolds stress data in the outer region of the wall jet

In the present study, for the Reynolds stress profiles in the outer layer, no explicit collapse was initially observed. By looking at the instantaneous velocity fields from the PIV images it can be seen that a return flow is clearly present in the region above the wall jet. This suggested application of the correction method proposed by Eriksson *et al*. (1998) on the Reynolds stress components in the outer layer. With this correction, a reasonable collapse of the Reynolds stress profiles in the outer layer was observed up to x/H = 100 in the current study. Note that the inner layer data should not be corrected since the correction method used for the outer layer will over-correct the velocity field in the inner layer according to Eriksson *et al*. (1998). Therefore, in the following figures, the corrected data was used whenever the outer scales were used for non-dimensionalization, and the un-corrected data was used when the inner scales were used for scaling.

2.2 The Reynolds stresses normalized by outer scales

Figure 5 shows the streamwise normal Reynolds stress profiles scaled using outer coordinates at the downstream location of x/H = 70 and 100 for both flow rates. In this figure, the present LFR data agree well with the data of Rostamy *et al*. (2011a) in the outer layer of the wall jet down to y_m, which would be expected since the present LFR slot Reynolds number of Re_o = 7250 is only 3% lower than the value used in their experiment. However, the present HFR profiles are clearly at a lower level than the LFR profiles, which indicates the dependence of the fluctuating velocity on the slot Reynolds number. This is in agreement with previous studies, for example, Wygnanski *et al*. (1992) found the magnitude of the peak streamwise Reynolds stress in the outer region at a downstream location would decrease as the slot Reynolds number was increased. In their Figure 6, Rostamy *et al*. (2011a) also confirmed this phenomenon. In addition, the self-similar behaviour of the streamwise Reynolds stress in the outer layer is evident for both flow rates in the present study. The profile for the HFR is close to that of both Abrahamsson *et al*. (1994) and Eriksson *et al*. (1998).

Figure 6 gives the profiles of the wall-normal Reynolds stress component in outer scales. Again, comparison with previous studies indicates a similar shape but different peak magnitudes for the Reynolds stress profiles. Within the measurement uncertainty, the present LFR profiles are in agreement with that of Rostamy *et al*. (2011a) in the outer layer down to $y/(y_{1/2})_{\text{out}} \approx 1.5$. The peak value of the present LFR profile is less than that from Rostamy *et al*. (2011a), however, the location of the peak value is $y/(y_{1/2})_{\text{out}} \approx 0.8$ which is in reasonable agreement with the value 0.75 reported by Rostamy *et al*. (2011a) and also close to the value 0.7 obtained by Eriksson *et al*. (1998). For the HFR data, the profiles in the outer layer are again lower in magnitude compared to the LFR case, while the location of the peak value is shifted slightly outwards to $y/(y_{1/2})_{\text{out}} \approx 1.0$. Similar to the streamwise case, the wall-normal Reynolds stress profiles exhibit self-similarity in the outer layer when scaled by outer coordinates for both flow rates. Note that although the slot Reynolds number of $\text{Re}_o = 1\times10^4$ used by Abrahamsson *et al*. (1994) is much lower than the present HFR condition, in the outer layer their data is significantly lower in magnitude than the present HFR profiles, which is different from the streamwise case (see Figure 5 above). As discussed by Rostamy *et al*. (2011a), this is probably due to the larger meansurement error in the fluctuating velocity field for HWA in the outer layer, especially for the wall-normal component.

The Reynolds shear stress profiles in outer scales are shown in Figure 7. The peak value is located at $y/(y_{1/2})_{\text{out}} \approx$ 0.75 and $y/(y_{1/2})_{\text{out}} \approx 0.8$ for the LFR and HFR, respectively, which is in good agreement with the value of $y/(y_{1/2})_{\text{out}}$ = 0.7 ~ 0.75 reported by Rostamy *et al*. (2011a). Self-similarity is observed for each flow rate, as for the other two Reynolds stress components. However, dependence on the slot Reynolds number is noticeably less than for the

$\langle u^2 \rangle$ and $\langle v^2 \rangle$ cases. The relatively low magnitude of the profile measured by Abrahamsson *et al*. (1994) is consistent with the inability of the HWA to accurately measure the wall-normal Reynolds stress component, as mentioned above.

George *et al*. (2000) concluded from a theoretical assessment that the normal Reynolds stresses in the outer flow scale with U_m^2, while the Reynolds shear stress collapses better with U_τ^2. However, the experimental data of Eriksson *et al*. (1998) and Rostamy *et al*. (2011a) did not support this theory. Figure 8 gives the present results for the Ryenolds shear stress re-plotted using U_τ^2 instead of U_m^2 to normalise the stress profile. It can be seen that scaling with U_τ^2 did improve the self-similarity in the outer region, however, but U_τ^2 was still unable to completely remove the Reynolds number dependency of the shear stress as suggested by George *et al*. (2000).

2.3 The turbulence quantities normalized by inner scales

The friction velocity U_τ and the inner length scale υ / U_τ were used as the inner scales to non-dimensionalize the fluctuating velocities in the inner layer of the wall jet. Figure 9 shows the profile of the dimensionless streamwise turbulence intensity as well as data from previous studies. The general shape of the present profile is similar to that measured in other studies. Again, a clear dependence on the slot Reynolds number Re_o is present. In addition, even at the same Re_o, i.e. for the same flow rate, the streamwise turbulence intensity profiles don't exhibit a self-similar pattern in the inner layer, but instead the level grows with distance from the slot exit, which indiates a local Reynolds number dependence. This is in agreement with the conclusion by Eriksson *et al*. (1998).

Figure 10 shows the profiles of the wall-normal turbulence intensity $< v^2 >^{1/2}$ non-dimensionalised with the friction velocity. Unlike the streamwise component $< u^2 >^{1/2}$, there is no twin-peak present in the inner layer for $< v^2 >^{1/2}$ profiles, but there does appear to be a weak inflection location at $y^+ \approx 40$. It can be seen that within the experimental error, the $< v^2 >^{1/2}$ profiles display a self-similar behaviour for each flow rate down to $y^+ \approx 300$, although the presence of the slot Reynolds number effect is still significant.

The profiles of the Reynolds shear stress scaled using inner coordinates for both flow rates are presented in Figure 11. Note that the PIV measurements could only obtain valid $< uv >$ data down to $y^+ \approx 100$, which is due to the inherent limitation of the current PIV instrumentation. As such, the present measurements do not resolve the negative peak value for the Reynolds shear stress close to the wall. Comparing to other studies, there is generally good agreement in terms of the trend of the data sets. The current LFR data closely follow the data of Rostamy *et al*. (2011a), while the HFR data are displaced below their results. Within the measurement uncertainty, the profiles for both flow rates show distinct self-similar patterns, which indicates a dependence on the slot Reynolds number. Although the present PIV measurements could not resolve the inner (minimum) peak of the Reynolds shear stress profile, the trend of the data (especially for the HFR case) suggests a location for the inner peak which is different from those reported by Eriksson *et al*. (1998) and Rostamy *et al*. (2011a). This may indicate that the inner peak exhibits some dependence on the slot Reynolds number, as observed by Rostamy *et al*. (2011a).

CONCLUSIONS

The present paper reports an experimental study of the fluctuating velocity fields of a plane turbulent wall jet on a smooth surface based on a new set of PIV measurements at two flow rates corresponding to slot Reynolds numbers of Re_o = 7250 and Re_o = 14400. Based on the mean velocity profiles, the fully developed region of the wall jet was determined to occur for downstream locations of $x / H \geq 40$ for both flow rates.

Due to the finite size of the experimental facility, the turbulence associated with the return flow outside the region of the wall jet was observed to erroneously enhance the level of the fluctuating velocities in the outer region. This effect was subsequently corrected for the outer region following the method used by Eriksson *et al*. (1998).

The present measurements gave similar yet in some ways distinct conclusions in comparison to previous studies. To study the self-similarity of the fluctuating velocity fields, the outer scales, i.e. the local maximum velocity U_m and the outer half-width $(y_{1/2})_{out}$, as well as the inner scales, i.e. the friction velocity U_τ and the viscous length scale υ / U_τ, were used to normalize the turbulence quantities following the theory of George *et al*. (2000). Self-similar behaviour was observed in the outer layer for all three components of the Reynolds stress when scaled with the outer scales, as well as for the wall-normal and shear stress profiles in the inner layer when scaled with the inner scales. A dependence on the slot Reynolds number was observed for all three Reynolds stress components, while the streamwise normal Reynolds stress additionally exhibited a dependence on the local Reynolds number, i.e. the streamwise location from the slot exit. The inner peak of the Reynolds shear stress profiles also exhibited a dependence on the slot Reynolds number.

Attention was also given to the conclusion of George *et al*. (2000) that the friction velocity U_τ would better collapse the shear stress profiles in the outer layer of the wall jet than the local maximum velocity U_m. For the present data, using U_τ improves the self-similarity of the resultant profiles, but some variations still persist.

ACKNOWLEDGEMENTS

The support of the Natural Sciences and Engineering Research Council of Canada is gratefully acknowledged.

REFERENCES

Abrahamsson, H., Johansson, B. and Lofdahl, L., 1994, "A turbulent plane two-dimensional wall jet in a quiescent surrounding", *European Journal of Mechanics - B/Fluids*, Vol. 13, pp. 533-556.

Barenblatt, G.I., Chorin, A.J., and Prostikishin, V.M, 2005, "The turbulent wall jet: A triple-layered structure and incomplete similarity". *Journal of Applied Mathematics*, Vol. 102, pp. 8850-8853.

Bradshaw, P. and Gee, M. T., 1960, "Turbulent Wall Jet with and without an External Stream," *Aerospace Research Council R&M* No. 3252.

Dejoan, A. and Leschziner, MA., 2005, "Large eddy simulation of a plane turbulent wall jet", *Physics of Fluids*, Vol. 17, 025102-1-16.

Dunn, M., 2010, "An experimental study of a plane turbulent wall jet using particle image velocimetry", *M.Sc. Thesis*, Department of Mechanical Engineering, University of Saskatchewan, Saskatoon.

Eriksson, J. G., Karlsson, R. I. and Persson, J., 1998, "An experimental study of a two-dimensional plane wall jet", *Experiments in Fluids*, Vol. 25, pp. 50-60.

George, W.K., Abrahamsson, H., Eriksson, J., Karlsson, R.I., Lofdahl, L., and Wosnik, M., 2000, "A similarity theory for the turbulent plane wall jet", *Journal of Fluid Mechanics*, Vol. 425, pp. 368-411.

Rostamy, N., Bergstrom, D. J., Sumner, D. and Bugg, J. D., 2010, "An experimental investigation of the skin friction in a plane turbulent wall jet over smooth and rough surfaces", *Proceedings of ASME 2010 3rd Joint US-European Fluids Engineering Summer Meeting and 8th International Conference on Nanochannels, Microchannels, and Minichannels (FEDSM2010-ICNMM2010)*, August 1-5, 2010, Montreal, Canada.

Rostamy, N., Bergstrom, D. J., Sumner, D. and Bugg, J. D., 2011a, "The effect of surface roughness on the turbulence structure of a plane wall jet", *Physics of Fluids*, Vol. 23, 085103-1.

Rostamy, N., Bergstrom, D. J., Sumner, D. and Bugg, J. D., 2011b, "An experimental study of a turbulent wall jet on smooth and transitionally rough surfaces", *ASME Journal of Fluids Engineering*, Vol. 133, 111207:1-8.

Shinneeb, A.M., 2006, "Confinement effects in shallow water jets", *Ph.D. Thesis*, Department of Mechanical Engineering, University of Saskatchewan, Saskatoon.

Tachie, M. F., 2001, "Open channel turbulent boundary layers and wall jets on smooth and rough surfaces," *Ph.D. Thesis*, Department of Mechanical Engineering, University of Saskatchewan, Saskatoon.

Tachie, M. F., Balachandar, R. and Bergstrom, D. J., 2004, "Roughness effects on turbulent plane wall jets in an open channel," *Experiments in Fluids*, Vol. 37, pp. 281-292.

Wygnanski, I., Katz, Y., and Horev, E., 1992, "On the applicability of various scaling laws to the turbulent wall jet," *Journal of Fluid Mechanics*, Vol. 234, pp. 669-690.

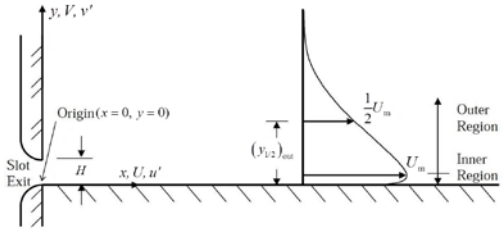

Figure 1. A schematic representation of a plane wall jet.

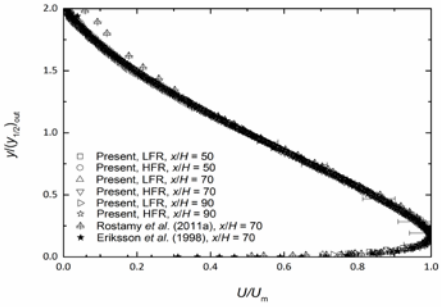

Figure 2. Streamwise mean velocity profile normalized by outer scales for LFR and HFR conditions.

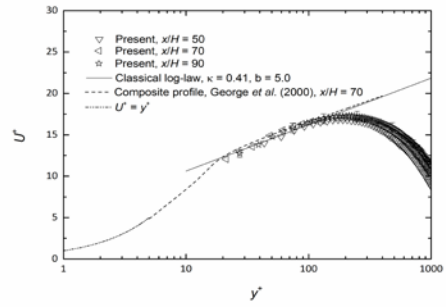

Figure 3. Streamwise mean velocity profile normalized by inner scales for LFR condition.

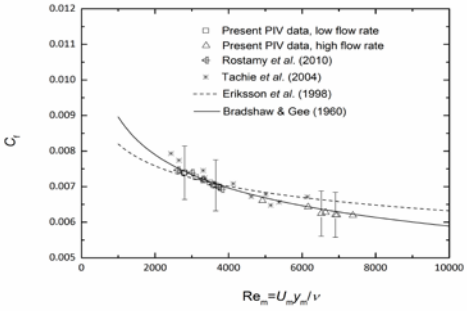

Figure 4. Variation of skin friction coefficient with local Reynolds number for LFR and HFR conditions.

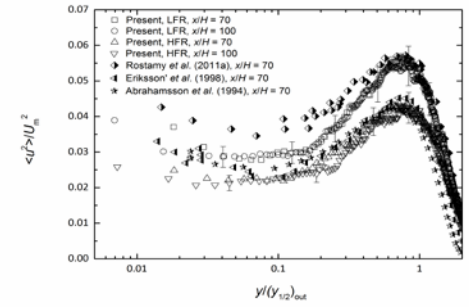

Figure 5. Streamwise Reynolds stress normalized by outer scales for LFR and HFR conditions (corrected data).

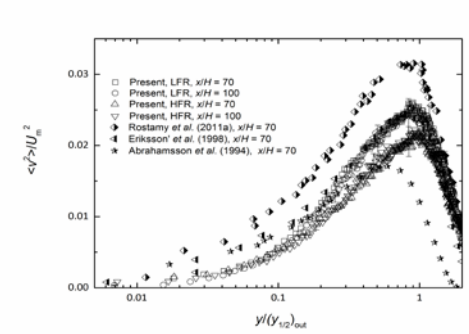

Figure 6. Wall-normal Reynolds stress normalized by outer scales for LFR and HFR conditions (corrected data).

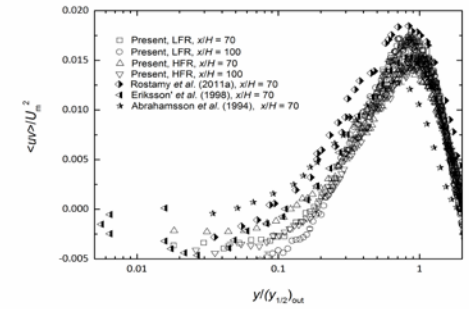

Figure 7. Reynolds shear stress normalized by outer scales for LFR and HFR conditions (corrected data).

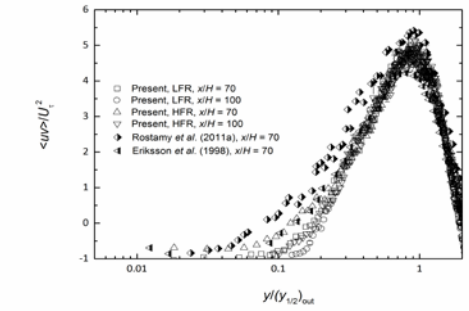

Figure 8. Reynolds shear stress normalized using inner velocity scale following George *et al.* (2000) (corrected data).

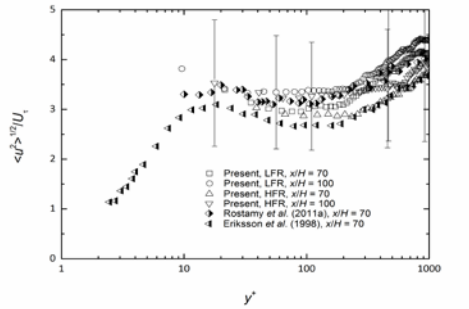

Figure 9. Streamwise turbulence intensity normalized by inner scales for LFR and HFR conditions (un-corrected data).

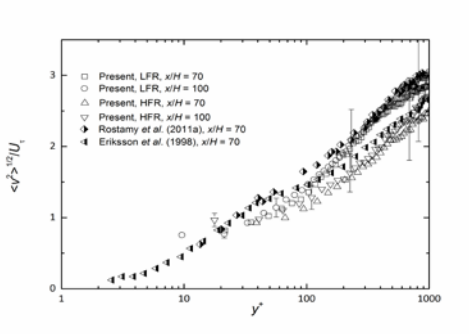

Figure 10. Wall-normal turbulence intensity normalized by inner scales for LFR and HFR conditions (un-corrected data).

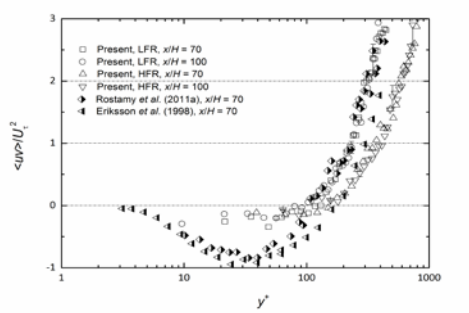

Figure 11. Reynolds shear stress normalized by inner scales for LFR and HFR conditions (un-corrected data).